Free-Carrier Absorption in n-Type Ge†*

ROBERT ROSENBERG AND MELVIN LAX
Bell Telephone Laboratories, Murray Hill, New Jersey

(Received June 19, 1958)

The structure of the conduction band of Ge is completely taken into account in calculating the cross section in second-order Born approximation. The second-order matrix element contains first-order matrix elements of electron-photon interaction (derived for anisotropic mass) and of electron-scatterer interaction. Scatterers considered are ionized impurities and phonons belonging to all six branches of the vibrational spectrum. Deformation parameters of electron-phonon interaction are chosen to agree with other experiments. An excellent fit to high-temperature data (450°K), where impurity effects are very small, is obtained without adjusting any parameters. Contributions to the cross section from processes involving scattering by longitudinal and transverse long-wavelength acoustic phonons are comparable; their combined effect is matched by energetic-phonon effects when $T \gtrsim 300$°K. In this temperature range, when $40\,\mu \gtrsim \lambda \gtrsim 10\,\mu$, contributions from all phonon processes are virtually indistinguishable in their temperature and wavelength (λ^2) dependence. Predicted cross sections are too low by 20–30% at 293°K, and by a factor of 2–4 at 78°K. The low-temperature results are in apparent disagreement with theoretical results of Fan, Spitzer, and Collins. It is suggested that their theory leads to an overestimate in the impurity calculation, and that impurity effects have not yet been explained.

1. INTRODUCTION

THE free-carrier absorption cross section σ_{FC} in n-type Ge is calculated here with full regard to current information on the structure of the conduction band. As is well known, the absorption of a photon by an electron in a perfect crystal is a forbidden process. The electron can gain a large amount of energy but very little momentum from the photon. In order for the absorption to occur, then, the electron must gain momentum from some lattice imperfection. This two-step process is accounted for in Sec. 2 by formulating the absorption cross section in second-order Born approximation. At this stage, the type of lattice imperfection which scatters the electron is left unspecified.

Two kinds of lattice imperfection are treated, namely phonons (Sec. 3) and ionized impurities (Sec. 4). All possible intraband electron transitions are discussed, i.e., intravalley transitions and intervalley transitions accomplished with or without the aid of an umklapp process. In the phonon case, the electron is allowed to interact with a phonon belonging to any of the six branches of the vibrational spectrum. Appropriate deformation parameters are assigned values in agreement with other properties[1] of n-type Ge, and comparison with the data of Fan, Spitzer, and Collins[2] (hereafter referred to as FSC) is made without adjusting any parameters. One may note that earlier[2–5] theories of free-carrier absorption all employ an adjustable effective mass for data fitting.

Section 5 summarizes the results and implications of the present theory.

2. FORMULATION OF FREE-CARRIER ABSORPTION CROSS SECTION

The free-carrier absorption cross section $\sigma_{FC}(\nu)$ is the ratio (net transition probability for absorption of a photon of energy $h\nu$ by a current carrier) ÷ (flux of photons of energy $h\nu$ through the crystal):

$$\sigma_{FC}(\nu) = [n(\mathbf{\nu},\alpha)c/\epsilon^{\frac{1}{2}}]^{-1}(W^a - W^e). \tag{2.1}$$

W^a is the transition probability for the absorption of a photon by a current carrier; W^e is the corresponding transition probability for *induced* photon emission[6]; $n(\mathbf{\nu},\alpha)$ is the beam density of photons having propagation vector $\mathbf{\nu}$ and polarization index $\alpha(\alpha = 1, 2)$; $c/\epsilon^{\frac{1}{2}}$ is the velocity of infrared photons in the crystal.

The transition probabilities are calculated in Born approximation with the aid of "golden rule number two,"

$$W = (2\pi/\hbar)\,\mathrm{Av}_0 \sum_f |M_{f0}|^2 \delta(E_f - E_0), \tag{2.2}$$

where Av_0 means the thermal average on initial states 0 and $\sum_f$ means the sum on final states f. M_{f0} is the second-order matrix element for a process in which an electron absorbs (or emits) a photon and is scattered by a scatterer, e.g., phonon, ionized impurity, etc. For definiteness, the transition probability (2.2) will be developed for the case of photon absorption, i.e., $W = W^a$, $M_{f0} = (M^a)_{f0}$; W^e is then obtained by making obvious changes in W^a.

The second-order matrix element $(M^a)_{f0}$ can be

† Supported in part by the Office of Naval Research.

* Part of a dissertation submitted by R. R. in partial fulfillment of the requirements for the degree of Doctor of Philosophy, in the Physics Department, Syracuse University, 1957.

[1] C. Herring, Bell System Tech. J. **34**, 237 (1955); C. Herring and E. Vogt, Phys. Rev. **101**, 944 (1956).

[2] Fan, Spitzer, and Collins, Phys. Rev. **101**, 566 (1956).

[3] H. Y. Fan and M. Becker, *Proceedings of the Reading Conference* (Butterworth Scientific Publications, Ltd. London, 1951), pp. 132–147. This article reviews both classical theory and the quantum-mechanical theory of H. Fröhlich.

[4] H. Schmidt, Z. Physik **139**, 433 (1954).

[5] B. Donovan and N. H. March, Proc. Phys. Soc. (London) **B70**, 883 (1957).

[6] Spontaneous emission is part of the background radiation. Schmidt's[4] theory is the first to recognize the necessity for subtracting of induced emission in the infrared,

written in abstract notation as follows: Denote the first-order photon absorption matrix element between electronic states $\mathbf{k}_B$, $\mathbf{k}_A$ by $(V_\nu^a)_{\mathbf{k}_B\mathbf{k}_A}\delta(\mathbf{k}_B,\mathbf{k}_A)$ [this form is derived in Appendix A—see (A.11)] and the first-order scattering matrix element by $(V_s)_{\mathbf{k}_B\mathbf{k}_A}$. Then $(M^a)_{f0}$ is the sum

$$(M^a)_{f0}=\sum_{\mathbf{k}_i}\left[\frac{(V_\nu^a)_{\mathbf{k}_f\mathbf{k}_i}\delta(\mathbf{k}_f,\mathbf{k}_i)(V_s)_{\mathbf{k}_i\mathbf{k}_0}}{E_0-E_i}+\frac{(V_s)_{\mathbf{k}_f\mathbf{k}_i}(V_\nu^a)_{\mathbf{k}_i\mathbf{k}_0}\delta(\mathbf{k}_i,\mathbf{k}_0)}{E_0-E_i'}\right], \quad (2.3)$$

on intermediate states i, where the brackets contain a sum on the two possible orders in which photon absorption and electron scattering can occur. The energy denominators in (2.3) are

$$E_0-E_i=E(\mathbf{k}_0)-E(\mathbf{k}_i)\pm E_s, \quad (2.4a)$$

$$E_0-E_i'=E(\mathbf{k}_0)-E(\mathbf{k}_i)+h\nu, \quad (2.4b)$$

where $\mathbf{k}_0$ and $\mathbf{k}_i$ are the initial and intermediate propagation vectors of the electron, and E_s is the energy which the electron gains from the scattering center or loses to it. The plus sign before E_s applies to a gain in electron energy, the minus sign to a loss.

Inserting the energy denominators (2.4) into Eq. (2.3) for $(M^a)_{f0}$, one can immediately sum on $\mathbf{k}_i$ to obtain

$$(M^a)_{f0}=(V_s)_{\mathbf{k}_f\mathbf{k}_0}\left[\frac{(V_\nu^a)_{\mathbf{k}_f\mathbf{k}_f}}{E(\mathbf{k}_0)-E(\mathbf{k}_f)\pm E_s}+\frac{(V_\nu^a)_{\mathbf{k}_0\mathbf{k}_0}}{h\nu}\right]. \quad (2.5)$$

The right-hand side of (2.5) can be further simplified by noting that (2.5) is to be used in conjunction with the energy conservation condition

$$\delta(E_f-E_0)=\delta[E(\mathbf{k}_f)-E(\mathbf{k}_0)-h\nu\mp E_s], \quad (2.6)$$

when one calculates the transition probability W^a according to the prescription (2.2). The first energy denominator on the right-hand side of (2.5) can therefore be replaced by $(-h\nu)$, so that $(M^a)_{f0}$ becomes

$$M_{f0}=(V_s)_{\mathbf{k}_f\mathbf{k}_0}[(V_\nu)_{\mathbf{k}_0\mathbf{k}_0}-(V_\nu)_{\mathbf{k}_f\mathbf{k}_f}]/h\nu. \quad (2.7)$$

Hence, for any scatterer which can be treated adequately in second-order Born approximation, the *first-order scattering matrix element between* initial *and* final *electron states appears as a factor in the second-order matrix element* M_{f0}. The absorption superscript a has been omitted from (2.7) because the matrix element $(M^e)_{f0}$ for induced photon emission is identical to $(M^a)_{f0}$.

It is now a simple matter to express the absorption cross section (2.1) in terms of first-order matrix elements. One introduces the second-order matrix element (2.7) and the energy conservation condition (2.6) into Eq. (2.2) to calculate the transition probability W^a for photon absorption. The transition probability W^e for induced photon emission is obtained by changing the sign of $h\nu$ in W^a. The W's are then put into the absorption cross section (2.1) to give

$$\sigma_{FC}(\nu)=(2\pi/\hbar)[n(\mathbf{v},\alpha)c/\epsilon^{\frac{1}{2}}]^{-1}\times\sum_s \mathrm{Av}_0\sum_f|(V_s)_{\mathbf{k}_f\mathbf{k}_0}|^2|(V_\nu)_{\mathbf{k}_0\mathbf{k}_0}-(V_\nu)_{\mathbf{k}_f\mathbf{k}_f}|^2(h\nu)^{-2}\times\sum_{p=0}^{1}(-1)^p\delta[E(\mathbf{k}_f)-E(\mathbf{k}_0)\mp E_s-(-1)^p h\nu]. \quad (2.8)$$

The summation on s runs over all types of scattering processes; the summation on p performs the subtraction W^a-W^e; the sign of E_s is that appropriate to a given scattering process.

The radiation part of the formulation (2.8) of $\sigma_{FC}(\nu)$ is now completed by inserting specific forms for $(V_\nu)_{\mathbf{k}_0\mathbf{k}_0}$ and $(V_\nu)_{\mathbf{k}_f\mathbf{k}_f}$. These matrix elements are derived in Appendix A under the assumption that the energy valleys can be described by a single mass dyadic for all states of importance to free-carrier absorption. This assumption will be valid provided that the electronic states of importance to free-carrier absorption lie within a set of ellipsoids, drawn about the energy minima in the Brillouin zone, whose axes are small compared with the radius of the Brillouin zone. An estimate of the size of these ellipsoids can be made with the aid of the energy conservation condition appearing in (2.8). From this condition, one obtains

$$E(\mathbf{k}_f)\lesssim(h\nu)_{\max}. \quad (2.9)$$

[The maximum value of $h\nu$ of interest here corresponds to a wavelength $\sim 10\,\mu$. Both $E(\mathbf{k}_0)$ and E_s correspond to much longer wavelengths. The initial electronic energy $E(\mathbf{k}_0)$ is $\sim kT$; on the wavelength scale, the room temperature value of kT lies at $\sim 50\,\mu$. As for the energy E_s exchanged with phonons or isolated impurity scatterers, the maximum phonon energy in Ge occurs at $\sim 35\,\mu$,[7] while the recoil energy of an isolated impurity is negligible.] Employing the cyclotron resonance mass[8] values in (2.9), one finds that the long semiaxis of the ellipsoids which bound the important final states is about two-tenths the radius of the Brillouin zone.

From (A.11), one obtains

$$(V_\nu)_{\mathbf{k}_0\mathbf{k}_0}=\gamma_0(\mathbf{v},\alpha)\boldsymbol{\varepsilon}(\mathbf{v},\alpha)\cdot\mathbf{m}_0^{-1}\cdot(\mathbf{k}_0-\mathbf{K}_0), \quad (2.10a)$$

$$(V_\nu)_{\mathbf{k}_f\mathbf{k}_f}=\gamma_0(\mathbf{v},\alpha)\boldsymbol{\varepsilon}(\mathbf{v},\alpha)\cdot\mathbf{m}_f^{-1}\cdot(\mathbf{k}_f-\mathbf{K}_f), \quad (2.10b)$$

where

$$\gamma_0(\mathbf{v},\alpha)=ie\hbar^2[2\pi n(\mathbf{v},\alpha)/(\epsilon h\nu)]^{\frac{1}{2}}; \quad (2.11)$$

$\boldsymbol{\varepsilon}(\mathbf{v},\alpha)$ is the unit polarization vector belonging to

[7] B. N. Brockhouse and P. K. Iyengar, Phys. Rev. **111**, 747 (1958). The estimate is actually $\sim 33\,\mu$.

[8] Dresselhaus, Kip, and Kittel, Phys. Rev. **98**, 368 (1955).

mode $(\mathbf{v},\alpha)$ of the radiation field, $\mathbf{m}_0^{-1}$ is the reciprocal mass dyadic of the initial valley whose minimum lies at $\mathbf{K}_0$, and $\mathbf{m}_f^{-1}$, $\mathbf{K}_f$ are the corresponding quantities in the final valley. (One sees from the arguments of the preceding paragraph that the important electronic states can be assigned unambiguously to one valley or another.)

From Eq. (2.10), one can form the expression

$$[n(\mathbf{v},\alpha)c/\epsilon^{\frac{1}{2}}]^{-1}|(V_\nu)_{\mathbf{k}_0\mathbf{k}_0}-(V_\nu)_{\mathbf{k}_f\mathbf{k}_f}|^2 = (\gamma_1/h\nu)\{[\mathbf{m}_0^{-1}\cdot(\mathbf{k}_0-\mathbf{K}_0)-\mathbf{m}_f^{-1}\cdot(\mathbf{k}_f-\mathbf{K}_f)]\cdot\boldsymbol{\varepsilon}(\mathbf{v},\alpha)\}^2, \quad (2.12)$$

where

$$\gamma_1=2\pi e^2\hbar^4/\epsilon^{\frac{1}{2}}c. \quad (2.13)$$

Before inserting (2.12) into the cross section (2.8), one can sum the dyadic $\boldsymbol{\varepsilon}(\mathbf{v},\alpha)\boldsymbol{\varepsilon}(\mathbf{v},\alpha)$ on the two values of the polarization index α and then average on all orientations of $\mathbf{v}$:

$$\langle\sum_{\alpha=1}^{2}\boldsymbol{\varepsilon}(\mathbf{v},\alpha)\boldsymbol{\varepsilon}(\mathbf{v},\alpha)\rangle_{\Omega_\nu}=\tfrac{1}{3}\mathbf{1}. \quad (2.14)$$

This procedure accounts for the unpolarized state of the incident beam and also yields the isotropy of the cross section in a cubic crystal. With (2.12) and (2.14) the cross section (2.8) becomes

$$\sigma_{FC}(\nu) = (2\pi/\hbar)[\gamma_1/3(kT)^4(2x)^3]\cdot\sum_s \mathrm{Av}_0\sum_f \times|(V_s)_{\mathbf{k}_f,\mathbf{k}_0}|^2[\mathbf{m}_0^{-1}\cdot(\mathbf{k}_0-\mathbf{k}_0)-\mathbf{m}_f^{-1}\cdot(\mathbf{k}_f-\mathbf{k}_f)]^2 \times\sum_{p=0}^{1}(-1)^p\delta\{[E(\mathbf{k}_f)-E(\mathbf{k}_0)]/kT\mp 2z-(-1)^p 2x\}, \quad (2.15)$$

where the definitions

$$2x=h\nu/kT, \quad 2z=E_s/kT \quad (2.16)$$

have been introduced for later convenience.

Equation (2.15) represents the furthest point to which one can carry the calculation of $\sigma_{FC}(\nu)$ without mentioning specific scattering mechanisms. One may note that the computation of $\sigma_{FC}(\nu)$ from (2.15) is simplified by expressing the average on initial states $\mathbf{k}_0$ and the sum on final states $\mathbf{k}_f$ in integral form; in addition, electronic energies are written

$$E(\mathbf{k}_A)=(\hbar^2/2)(\mathbf{k}_A-\mathbf{K}_A)\cdot\mathbf{m}_A^{-1}\cdot(\mathbf{k}_A-\mathbf{K}_A). \quad (2.17)$$

3. PHONON SCATTERERS

In treating the effect of electron-phonon collisions on $\sigma_{FC}(\nu)$, one must consider all the different types of scattering matrix element $(V_s)_{\mathbf{k}_f\mathbf{k}_0}$ permitted by the location of the energy valleys in the Brillouin zone and by the vibrational spectrum of Ge. Briefly, the presence of a number of well separated valleys allows intravalley transitions ($\mathbf{k}_f$ and $\mathbf{k}_0$ in the same valley) and intervalley transitions of two kinds. Direct and indirect intervalley transitions can readily be understood when one recalls that the final electronic momentum $\hbar\mathbf{k}_f$ is the sum of phonon and initial electronic momenta $\hbar\boldsymbol{\tau}+\hbar\mathbf{k}_0$. (Photon momentum is negligible.) Some phonons of large momentum are suitably oriented so that the electron is scattered directly from one valley into another. Other phonons are so oriented that $(\boldsymbol{\tau}+\mathbf{k}_0)$ falls outside the (reduced) Brillouin zone. In this case, the final electron state $\mathbf{k}_f$ is brought to a new valley inside the zone by an umklapp process, i.e., by addition of a reciprocal lattice vector $\boldsymbol{\kappa}$. Figure 1 shows how final electron states fill the Brillouin zone when the electron starts from a given initial state. The filling is seen to be unique; a transition between two definite electron states proceeds either directly ($\boldsymbol{\kappa}=0$) or by the only available indirect process ($\boldsymbol{\kappa}\neq 0$).

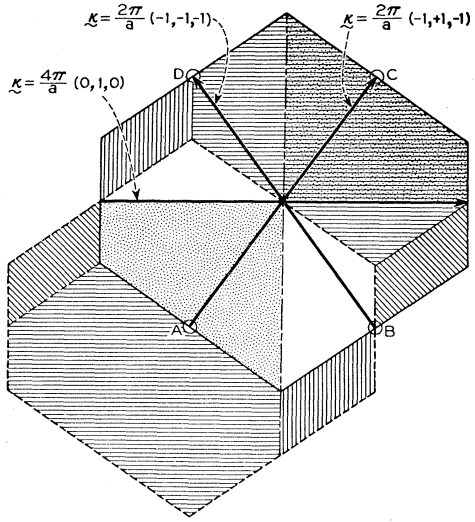

FIG. 1. Filling of the Brillouin zone. It is shown how the electronic Brillouin zone is completely and uniquely filled by final states under phonon transitions starting from the energy minimum at $\mathbf{K}_A=(\pi/a)(1,1,1)$. The solid hexagon is the cross section of the electronic zone in the $(-1,0,1)$ plane passing through the zone origin. With the initial electronic state at the minimum A, the points B, D, and C are respectively the first-, second-, and third-neighbor minima. The stippled areas are those which lie in the initial octant of the Brillouin zone and the third-neighbor octant. The unstippled areas belong to first- and second-neighbor octants. The dashed hexagon represents the phonon Brillouin zone whose origin has been placed at the initial state A. The phonon propagation vector $\boldsymbol{\tau}$ must lie within this hexagon. The horizontally lined area of the phonon zone is the region in which $\boldsymbol{\tau}$ has values such that $\mathbf{K}_A+\boldsymbol{\tau}+(2\pi/a)(-1,1,-1)$ falls in the horizontally lined area of the electronic zone. The other lined areas correspond to analogous umklapp processes; the vertical lines go with the umklapp vector $\boldsymbol{\kappa}=(2\pi/a)(-1,-1,-1)$ and the diagonal lines with $\boldsymbol{\kappa}=(4\pi/a)(0,1,0)$. The unlined area of the electronic zone is the region of overlap with the phonon zone, i.e., only direct ($\boldsymbol{\kappa}=0$) transitions occur here.

In addition to these complications, the phonon itself can belong to any of the six branches of the vibrational spectrum.

Despite the profusion of disinguishable types of electron-phonon scattering process, it is possible to

represent the appropriate matrix elements by only two general forms. Derivation of the matrix elements is a lengthy affair, and will be reserved for a separate paper on a generalized deformation-potential theory. Certain results useful in the present work will simply be quoted here. For the sake of plausibility, the connection with Bardeen and Shockley's[9] deformation-potential theory will be made.

Typical of the scattering matrix elements $(V_s)_{f0}$ to be used in the cross-section formulation (2.15) is the matrix element $(V_\tau{}^a)_{f0}$ for electron scattering via phonon absorption (superscript a):

$$(V_\tau{}^a)_{f0}=\left[\frac{\hbar N(\tau,t)}{2\rho V\omega(\tau,t)}\right]^{\frac{1}{2}}\delta(\mathbf{k}_f,\mathbf{k}_0+\tau+\kappa)\varepsilon(\tau,t)\cdot\mathbf{Y}(\tau,t), \quad (3.1)$$

where τ is the phonon propagation vector and t is the branch[10] index of the mode; $N(\tau,t)$, $\hbar\omega(\tau,t)$, $\varepsilon(\tau,t)$ are respectively the (equilibrium) excitation number, energy and unit polarization vector of mode (τ,t); V and ρ are the volume and density of the crystal. Except for $\mathbf{Y}$, all the factors on the right-hand side of (3.1) are immediately recognizable from the Bardeen-Shockley[9] theory. The "interaction vectors" $\mathbf{Y}(\tau,t)$ embody the generalization of their theory to a many-valley band. As one might expect, $\mathbf{Y}$ contains a deformation parameter which measures the strength of electron-phonon interaction in each type of scattering process. For the simple band structure treated by Bardeen and Shockley, $\mathbf{Y}$ reduces to their value $E_1\tau$.

For the present many-valley case, the following approximate forms of the interaction vector $\mathbf{Y}$ result from the generalization of deformation-potential theory:

Long-wavelength acoustic modes.—

$$\mathbf{Y}(\tau,t)=[A_1\mathbf{1}+A_2(3\mathbf{e}_0\mathbf{e}_0-\mathbf{1})]\cdot\tau, \quad (3.2)$$

$$\mathbf{e}_0=\mathbf{K}_0/K_0. \quad (3.3)$$

Energetic modes.—

$$\mathbf{Y}(\tau,t)=\mathbf{B}_n(\mathbf{K}_f,\mathbf{K}_0). \quad (3.4)$$

The subscript n on $\mathbf{B}_n$ runs over enough integers to encompass all the types of energetic-mode scattering. The value $n=0$ is reversed for scattering by long-wavelength optical modes; the remaining values of n apply to scattering by shorter wavelength modes.

The matrix element $(V_\tau{}^e)_{f0}$ for electron scattering via phonon emission is obtained from $(V_\tau{}^a)_{f0}$, Eq. (3.1), by replacing $N(\tau,t)$ with $N(\tau,t)+1$ and by changing the sign of τ in the Kronecker delta.

When one calculates the absorption cross section (2.15) with the aid of the electron-phonon matrix elements (3.1), one meets a complication which has not yet been discussed: Because the conduction band minima in Ge most probably lie on the zone boundary, one should, in principle, average the initial electron states and sum the final electron states on domains bounded by the surface of the Brillouin zone. On the other hand, one would like to perform the equivalent integrations on unrestricted domains. It turns out that the latter procedure is correct for scattering by long-wavelength phonons in Ge. For these phonons, third-neighbor indirect scattering processes are indistinguishable from intravalley processes. Both types of scattering are exactly taken into account if one integrates intravalley processes on complete valleys. The integrations can also be performed on complete valleys in calculating the remaining (intervalley) contributions to $\sigma_{FC}(\nu)$. These contributions have a wavelength and temperature dependence which is quite insensitive to the exact limitations on the domains of integration. These contributions are furthermore indistinguishable from that due to long-wavelength optical modes at temperatures at which phonons are the dominant scatterers. For the purpose of comparison with experiment, then, there will be no need to consider fine details of the different energetic-mode contributions.

The contributions to $\sigma_{FC}(\nu)$ made by the various phonon processes can now be computed from the cross-section formula (2.15), the scattering matrix elements (3.1), and the interaction vectors (3.2) and (3.4), with the aid of a few physical approximations discussed in Appendix B. The resulting phonon contribution $\sigma_{FC}{}^P(\nu)$ to the total cross section follows:

$$\sigma_{FC}{}^P(\nu)=\sum_{m=1}^{3}\sigma_m(\nu), \quad (3.5)$$

$$\sigma_1(\nu)=\Gamma_1(kT)^{-\frac{1}{2}}x^{-1}\sinh(x)K_2(x), \quad (3.6)$$

$$\sigma_2(\nu)/\sigma_1(\nu)=\Gamma_2/\Gamma_1, \quad (3.7)$$

$$\sigma_3(\nu)/\sigma_1(\nu)=\varphi(\omega_\tau)f_1{}^{-1}(\beta)(\hbar v_T/\Omega_c{}^{\frac{1}{2}})^2 z_\tau(\sinh z_\tau)^{-1}$$
$$\times\frac{(1+\xi)^2K_2[x(1+\xi)]+(1-\xi)^2K_2[x|1-\xi|]}{2K_2(x)}, \quad (3.8)$$

where $K_2(x)$ is the modified Bessel functions as defined by Watson,[11] and

$$2z_\tau=\hbar\omega_\tau/kT, \quad (3.9a)$$

$$\xi=z_\tau/x. \quad (3.9b)$$

The contributions σ_1 and σ_2 arise from processes involving, respectively, transverse and longitudinal long-wavelength acoustic phonons; σ_3 lumps together all energetic-mode contributions. This lumping is justified by the numerical values of the ratio σ_3/σ_1, Eq. (3.8). Despite appearances, the right-hand side of

[9] J. Bardeen and W. Shockley, Phys. Rev. **80**, 72 (1950).

[10] $t=1,2,3$: acoustic branches
4,5,6: optical branches
3,6: longitudinal branches
1,2,4,5: transverse branches

[11] G. N. Watson, *A Treatise on the Theory of Bessel Functions* (The Macmillan Company, New York, 1945), second edition, p. 78.

(3.8) is effectively independent of wavelength and temperature when $\lambda \lesssim 40\,\mu$ and when T is large enough ($\gtrsim 300°\mathrm{K}$) to make phonons the dominant scatterers. This behavior is a consequence of the long wavelength, $\sim 35\,\mu$, of the Raman line in Ge. The parameters which carry the phonon index τ in (3.8) will therefore be interpreted as referring to some mean mode whose energy and deformation parameter fit a number of experiments.

The constants Γ_1 and Γ_2 in (3.6) and (3.7) are

$$\Gamma_1=\frac{4}{3}\frac{e^2}{\hbar c}\left(\frac{2\det\mathbf{m}}{\pi\epsilon}\right)^{\frac{1}{2}}\frac{\langle\mathbf{m}^{-1}\rangle f_1(\beta)\Xi_u^2}{\hbar\rho v_T^2}, \tag{3.10a}$$

$$\frac{\Gamma_2}{\Gamma_1}=\left(\frac{v_T}{v_L}\right)^2 f_1^{-1}(\beta) \times\left[\left(\frac{\Xi_d}{\Xi_u}\right)^2+\frac{\Xi_d}{\Xi_u}f_2(\beta)+\tfrac{1}{2}f_2(\beta)-f_1(\beta)\right], \tag{3.10b}$$

where v_T and v_L are respectively the velocities of sound for transverse and longitudinal modes. Equations (3.10a,b) are expressed in terms of deformation parameters defined by Herring[1] and Vogt. The relations between their parameters Ξ_d, Ξ_u, and the deformation energies A_1, A_2 which appear in the interaction vector (3.2) are

$$\Xi_u=3A_2, \tag{3.11a}$$

$$\Xi_d=A_1-A_2. \tag{3.11b}$$

Also,[8]

$$(\det\mathbf{m})=m_1m_2^2=1.58(0.082)^2m^3=0.011m^3, \tag{3.12a}$$

$$\langle\mathbf{m}^{-1}\rangle=\tfrac{1}{3}(m_1^{-1}+2m_2^{-1})=8.3m^{-1}, \tag{3.12b}$$

$$\beta=m_2/m_1=0.052. \tag{3.12c}$$

The functions $f_1(\beta)$ and $f_2(\beta)$ come from angular integrations which enter the cross section (2.15) through the mass-dependent part of the electron-photon matrix element (A.11), and through the orientational restriction imposed by the Kronecker delta of the electron-phonon matrix element (3.1). The integrations are on orientations of the unit vector $\mathbf{u}=(\mathbf{k}_f-\mathbf{k}_0)\cdot\mathbf{m}^{-\frac{1}{2}}/|(\mathbf{k}_f-\mathbf{k}_0)\cdot\mathbf{m}^{-\frac{1}{2}}|$:

$$f_1(\beta)\equiv(4\pi\langle\mathbf{m}^{-1}\rangle)^{-1}\int d\Omega_u(\mathbf{u}\cdot\mathbf{m}^{-1}\cdot\mathbf{u})(\alpha_u^2-\alpha_u^4)$$

$$=\frac{\frac{3}{2}}{(2+\beta)(1-\beta)^2}\left[(1+5\beta+2\beta^2)\left(\frac{\beta}{1-\beta}\right)^{\frac{1}{2}}\times\tan^{-1}\left(\frac{1-\beta}{\beta}\right)^{\frac{1}{2}}-\frac{\beta}{3}(13+11\beta)\right]$$

$$=0.132, \tag{3.13}$$

$$f_2(\beta)\equiv(2\pi\langle\mathbf{m}^{-1}\rangle)^{-1}\int d\Omega_u(\mathbf{u}\cdot\mathbf{m}^{-1}\cdot\mathbf{u})\alpha_u^2$$

$$=\frac{6(1+\beta)}{(2+\beta)(1-\beta)}\left[1-\frac{1}{3}\left(\frac{1-\beta}{1+\beta}\right)-\left(\frac{\beta}{1-\beta}\right)^{\frac{1}{2}}\times\tan^{-1}\left(\frac{1-\beta}{\beta}\right)^{\frac{1}{2}}\right]$$

$$=1.25, \tag{3.14}$$

where

$$\alpha_u\equiv\mathbf{e}_0\cdot\mathbf{m}^{\frac{1}{2}}\cdot\mathbf{u}/|\mathbf{m}^{\frac{1}{2}}\cdot\mathbf{u}|. \tag{3.15}$$

The function $\varphi(\omega_\tau)$ which occurs in the energetic-mode contribution (3.8) is the combination

$$\varphi(\omega_\tau)=(B_\tau\Omega_c^{\frac{1}{3}}/\Xi_u)^2(\hbar\omega_\tau)^{-2} \tag{3.16}$$

of deformation parameters and phonon energy which is most conveniently evaluated from Herring's[1] work. The volume Ω_c of unit (two-particle) cell has been introduced to form certain quantities with dimensions of energy in (3.8) and (3.16). [Comparison of the interaction vectors (3.2) and (3.4) shows that the $\mathbf{B}$'s must have the dimensions of force since the A's are energies.]

Before the result (3.5)–(3.8) can be compared with experiment, one needs numerical values of the deformation parameters Ξ_u, Ξ_d and the function $\varphi(\omega_\tau)$ defined in (3.16), the velocities of sound v_T and v_L, and the normalized phonon energy $2z_\tau$.

The deformation parameters Ξ_u and Ξ_d for acoustic modes have been selected from Herring and Vogt's paper[1] on transport properties in many-valley semiconductors. Piezoresistance and magnetoresistance information lead to the choice

$$\Xi_u=16.4\text{ ev}, \tag{3.17a}$$

$$\Xi_d/\Xi_u=-0.23. \tag{3.17b}$$

Any other choice which is in reasonable agreement with the aforementioned information and with the shift of band gap with dilatation will lead to nearly the same values of absorption cross section as do (3.17a) and (3.17b).

The function $\varphi(\omega_\tau)$, Eq. (3.16), has been evaluated by combining Herring and Vogt's[1] analysis with Herring's[1] treatment of energetic-mode scattering based on an isotropic electron relaxation time. If Herring's ratio w_2/w_1 (relative strength of energetic mode to long-wavelength acoustic mode scattering) is chosen to be $\frac{1}{3}$, one finds

$$\varphi(\omega_\tau)\simeq 1.3\times10^{27}\text{ erg}^{-2}. \tag{3.18}$$

The velocities of sound which enter the constants (3.10a,b) actually come in as mean values on v_T^{-2} and

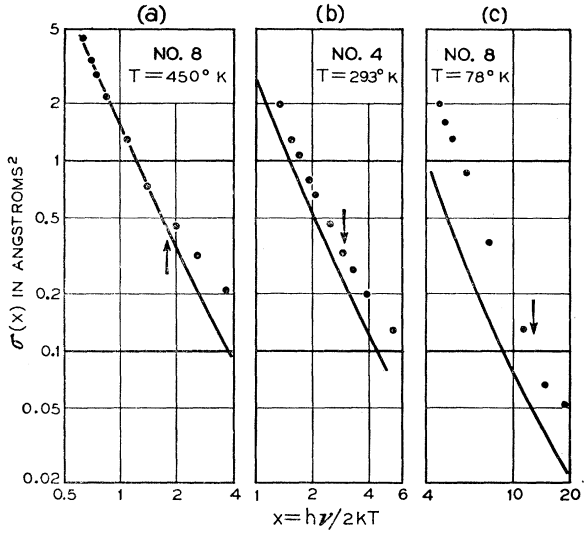

FIG. 2. Comparison of the calculated cross section with the data of Fan, Spitzer, and Collins.[2] The points are experimental free-carrier absorption cross sections reported by FSC for typical samples numbered 4 and 8. The curves have been calculated theoretically from Eqs. (3.5)–(3.8), (3.10), (3.13), (3.14), and (3.16) for phonon processes and from (4.4), (4.6), and (4.11) for ionized impurity processes. To the right of the arrows, Herman's[15] estimate of a 0.18-ev energy separation between [111] and [100] minima in Ge leads one to expect additional absorption, not included in the present theory, due to electronic transitions to [100] valleys.

v_L^{-2}. The values

$$v_T^{-2}=10^{-11}\ (\text{cm/sec})^{-2}, \tag{3.19a}$$

$$v_L^{-2}/v_T^{-2}=0.36, \tag{3.19b}$$

employed here have been averaged by the method of Quimby and Sutton[12] with the aid of room-temperature values of the elastic constants measured by McSkimin.[13]

The results (3.19) are rather insensitive to whether the mean is taken in all directions of propagation or only on selected directions.

The energy $\hbar\omega_\tau$ has been chosen to agree with the fundamental optical vibration somewhere near 35 μ.[7] One thus employs the maximum possible value of z_τ in the energetic-mode contribution (3.8) to the cross section. Nevertheless, one finds that to within an accuracy of a few percent, the factor $z_\tau(\sinh z_\tau)^{-1}$ and the factor in curly braces in (3.8) are both unity at room temperature and above in the experimental wavelength range.

With the above numbers, transverse and longitudinal long-wavelength acoustic modes contribute about equally to the absorption cross section, and their combined contribution is matched by energetic-mode scatterers at room temperature and above. In this range $\sigma_{FC}{}^P(\nu)$ varies almost exactly as λ^2.

Figure 2 (a) compares the calculated cross section (3.5–8) with the data of FSC under conditions where impurity scattering is relatively unimportant. *Note that the excellent fit has been obtained without adjusting any parameters.* The parameters are those which agree with other measured properties of Ge. If one accepts this fit as a verification of the phonon calculation, the burden of the discrepancies at 293°K and 78°K, Figs. 2 (b,c), falls upon some other scattering mechanism. This suggestion will be discussed after the calculation of impurity effects.

The arrows in Figs. 2 (a)–(c) are seen to occur at the noticeable break in the observed cross sections. The positions of the arrows indicate where one expects the next higher conduction band to provide additional states into which an electron can be scattered. [From the observed[14] variation of optical absorption edge with composition in Ge—Si alloys, Herman[15] estimates that the [100] minima in Ge lie about 0.18 ev above the [111] minima. The arrows have been drawn where $h\nu=0.18$ ev$-kT$.] No attempt has been made here to take these additional states into account. Hence, the divergence of high-temperature theoretical and experimental results at the arrow is in agreement with the estimated energy gap between [111] and [100] minima.

4. IONIZED IMPURITY SCATTERERS

An estimate of the effect of ionized impurity scattering on the free-carrier absorption cross section can be made by using the same formalism as for phonon scattering. Starting with the cross-section formula (2.15) derived in second Born approximation, one inserts the first-order scattering matrix element $(V_s)_{\mathbf{k}_f\mathbf{k}_0}$ and the transferred scatterer energy $2z$ and makes the calculation. This procedure is apparently too naive, as one sees from Fig. 2 (c). The resulting theoretical curve is too low by a factor of 2–4, and furthermore has the wrong wavelength dependence at a temperature $T=78$°K, where ionized impurity effects may be expected to predominate.

The above conclusions stand in apparent contradiction to the work of FSC,[2] who feel that impurity effects are understood. A brief sketch of the present calculation of $\sigma_{FC}{}^I(\nu)$ (index I means ionized impurity scatterers) will therefore be given, and the contradiction will subsequently be discussed.

The scattering matrix element,

$$(V_I)_{f0}=\pm(4\pi e^2/\epsilon V)f_0[(\mathbf{k}_f-\mathbf{k}_0)^2+\delta^2]^{-1}, \tag{4.1}$$

used in the present treatment is the matrix element of the screened Coulomb potential,

$$U=\pm(e^2/\epsilon)r^{-1}\exp(-\delta r), \tag{4.2}$$

taken between electronic Bloch waves belonging to states $\mathbf{k}_f$ and $\mathbf{k}_0$. The factor ϵ^{-1} accounts for dielectric shielding; the screening radius δ^{-1} is given the familiar

[12] S. L. Quimby and P. M. Sutton, Phys. Rev. **91**, 1122 (1953).
[13] H. J. McSkimin, J. Appl. Phys. **24**, 988 (1953).
[14] E. R. Johnson and S. M. Christian, Phys. Rev. **95**, 560 (1954).
[15] G. Herman, Phys. Rev. **95**, 847 (1954).

Debye-Hückel form

$$\delta^2=4\pi n_c e^2/(\epsilon kT), \tag{4.3}$$

where n_c is the concentration of free carriers.

In general, the matrix element (4.1) should be written as a summation on reciprocal lattice vectors $\boldsymbol{\kappa}$ of the expression $f_{\boldsymbol{\kappa}}[(\mathbf{k}_f-\mathbf{k}_0-\boldsymbol{\kappa})^2+\delta^2]^{-1}$, where $f_{\boldsymbol{\kappa}}$ is the κth Fourier component of the product of periodic parts of the Bloch waves. The term $\boldsymbol{\kappa}=0$ happens to be sufficient in the present calculation for the following reasons. Just as in the phonon case, intravalley ($\boldsymbol{\kappa}=0$) and third-neighbor intervalley ($\boldsymbol{\kappa}=\mathbf{k}_f-\mathbf{k}_0$) processes are complementary when the energy minima lie on the zone boundary. In addition, all other processes can be shown to be negligible. Hence, $\sigma_{FC}{}^I(\nu)$ is obtained by using just the matrix element (4.1) for the case $\boldsymbol{\kappa}=0$ in the cross section (2.15) and performing the sum on $\mathbf{k}_f$ and the average on $\mathbf{k}_0$ on unrestricted domains. When this procedure[16] is followed, one finds that all integrals but the last can be evaluated in closed form. In terms of the final integral, the cross section (2.15) becomes

$$\sigma_{FC}{}^I(\nu)=\Gamma_I(kT)^{-7/2}x^{-3}\sinh(x)F(x,\Delta^2,b), \tag{4.4}$$

where x is the normalized photon energy defined in (2.16), b^{-1} is the mass parameter β defined in (3.12c), and

$$\Delta^2=\hbar^2\delta^2/(2m_2kT), \quad m_2=0.082m. \tag{4.5}$$

The constant coefficient

$$\Gamma_I=\tfrac{1}{3}(2\pi)^{3/2}|f_0|^2n_I e^6\hbar^2/[c\epsilon^{5/2}(\det\mathbf{m})^{1/2}] \tag{4.6}$$

contains the density n_I of ionized impurities because one must count all scattering centers whose potential is (4.2).

The complicated function F in (4.4) is

$$F(x,\Delta^2,b)=\tfrac{1}{2}G(0)(b-1)^{-1}\cdot\int_0^\infty\frac{d\eta}{\eta}\times\exp\left[-\frac{x}{2}\left(\eta+\frac{1}{\eta}\right)\right]\left[G\left(\frac{\eta}{X}\right)\Big/G(0)\right], \tag{4.7}$$

where

$$G(y)=(1+y)^{-1}\left\{(b-1)(b+1+y)(b+y)^{-1}+(b-1-y)\left(\frac{b-1}{1+y}\right)^{\frac{1}{2}}\tan^{-1}\left(\frac{b-1}{1+y}\right)^{\frac{1}{2}}\right\}, \tag{4.8}$$

$$X=2x/\Delta^2. \tag{4.9}$$

The form (4.8) of $G(y)$ has been accurately approximated on the interval $0\leq y\leq b-1$ by a sum of decreasing exponentials:

$$G(\eta/X)/G(0)=0.476\exp(-2.4\eta/X)+0.443\exp(-0.68\eta/X)+0.081\exp(-0.13\eta/X). \tag{4.10}$$

The approximation (4.10) enables one to evaluate the integral in F, (4.7), in closed form to within a 5% error (probably smaller) in the parameter ranges $T\lesssim 300°\text{K}$, $n_c\lesssim 10^{18}$ cm^{-3}, $\lambda\lesssim 50\,\mu$. The function F defined in (4.7) is thus

$$F(x,\Delta^2,b)\simeq G(0)(b-1)^{-1}\times\{0.476K_0[(x^2+2.4\Delta^2)^{\frac{1}{2}}]+0.443K_0[(x^2+0.68\Delta^2)^{\frac{1}{2}}]+0.081K_0[(x^2+0.13\Delta^2)^{\frac{1}{2}}]\}, \tag{4.11}$$

where K_0 is a modified Bessel function as defined by Watson.[11] The present evaluation of $\sigma_{FC}{}^I(\nu)$ is given by the cross section (4.4) with the constant Γ_I and the auxiliary function $F(x,\Delta^2,b)$ given respectively by (4.6) and (4.11). Figure 3 is a plot of the product $G^{-1}(0)(b-1)$

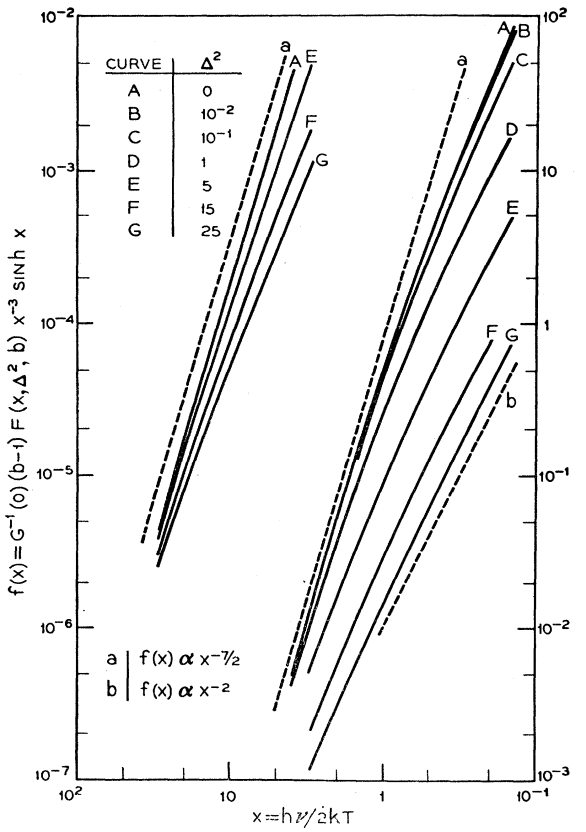

FIG. 3. Plot of $f(x)=G^{-1}(0)(b-1)F(x,\Delta^2,b)x^{-3}\sinh x$ *vs* $x=h\nu/2kT$. The part $\sigma_{FC}{}^I$ of the free carrier absorption cross section which arises from scattering by ionized impurities has the wavelength dependence of $f(x)$ according to the present calculation, where the parameter for the family of curves is $\Delta^2=\hbar^2\delta^2/2m_2kT$, δ is the inverse screening radius given by (4.3), and m_2 is the small principal mass of the conduction band. $F(x,\Delta^2,b)$ is given by (4.11). The parameter b is the reciprocal of β (3.12c). The constant $G(0)$ is found from (4.8). The two groups of curves are scaled according to the nearest ordinate, and connect smoothly.

[16] The transferred scatterer energy $2z$ is omitted from the energy conservation condition in the cross section (2.15) because of the negligible size of the ion's recoil energy.

$\times F(x,\Delta^2,b)x^{-3}\sinh x[=G^{-1}(0)(b-1)\Gamma_I^{-1}(kT)^{7/2}\sigma_{FC}{}^I(\nu)]$ *vs* x for a variety of values of Δ^2 which span the data of FSC.[2] One sees that for large x (short wavelengths and/or low temperatures), all the curves asymptotically approach the $\lambda^{7/2}$ behavior typical of unscreened ions. For smaller values of x, an increase in screening (i.e., in Δ^2) drastically reduces the value of the function, and the curves asymptotically approach the λ^2 behavior typical of phonon effects.

In plotting the curves of Figs. 2 (a)–(c), it has been assumed that f_0 [see (4.6)], the overlap integral of the periodic parts of two Bloch waves, is unity. The true value is probably smaller, which would only make the fit at $T=293$°K and 78°K poorer.

The comparison of theory and experiment leads the writers to believe that phonon effects on free-carrier absorption are satisfactorily understood while ionized-impurity effects are not. It is clear from the first three figures of FSC[2] that impurity effects are negligible at 450°K but not at 293°K and 78°K. At the latter two temperatures, the experimental cross sections show a marked increase with increasing impurity concentration. At 450°K, where theory and experiment are in excellent agreement, the experimental cross sections are virtually independent of impurity concentration.

The partial agreement which FSC[2] achieve between theory and experiment at lower temperatures can be explained as follows. Examination of Fig. 2(c) shows that one has to increase both magnitude and slope of the theoretical curve to improve agreement with the data. Both types of increase are appreciable when one neglects screening entirely (see Fig. 3), as did FCS. FSC also get an increase in slope by neglecting induced emission of photons, which offsets photon absorption most strongly at long wavelengths. Another increase in magnitude enters FSC's theory through their adjustable mass parameter m^*. Their selected value of m^* yields a 25% increase in the calculated cross section above the cross section produced by the "correct" effective mass. The "correct" mass can be found from the present results [(4.4), (4.6), and (4.11)] by ignoring screening and proceeding to the limit of isotropic mass; one obtains

$$2/m^{*\frac{3}{2}}=\lim_{b\to 1}[(\det\mathbf{m})^{-\frac{1}{2}}G(0)/(b-1)], \quad (4.12)$$

or

$$m_{\text{present}}{}^*/m=0.096, \quad (4.13a)$$

while

$$m_{FSC}{}^*/m=0.083. \quad (4.13b)$$

For these reasons, and because of other objections[17–19] which have been raised against treating low-temperature impurity effects in Born approximation, the writers believe that a valid calculation of $\sigma_{FC}{}^I(\nu)$ has not yet been done.

[17] R. Wolfe, Proc. Phys. Soc. (London) **A67**, 74 (1954).
[18] N. Sclar, Phys. Rev. **104**, 1548 (1956).
[19] F. J. Blatt, J. Phys. Chem. Solids **1**, 262 (1957).

5. SUMMARY

The observed free-carrier absorption cross section in Ge has been satisfactorily explained at high temperatures without adjusting any parameters. Parameters which appear in the present work are chosen to agree[1] with other experiments. Theory and experiment at 450°K indicate that impurity effects are negligible at this temperature. About half the cross section at 450°K arises from processes involving scattering by long-wavelength acoustic modes: energetic-mode scattering is responsible for the remaining half. Contributions to $\sigma_{FC}(\nu)$ from the various types of phonon scattering processes all have the same wavelength and temperature dependence above room temperature in the experimental wavelength range.

At room temperature and below, impurity scattering has a significant effect on $\sigma_{FC}(\nu)$. It appears that no no adequate theory of this effect exists.

ACKNOWLEDGMENT

The writers are indebted to Dr. R. J. Collins for enlightenment on experimental aspects of the problem.

APPENDIX A

Matrix elements are derived here for the interaction between a photon and an electron which lies in valley A of a many-valley band. For the sake of brevity, the effective mass approximation is employed. In this approximation, the unperturbed Hamiltonian H^0 near an energy minimum at $\mathbf{K}_A$ is

$$H^0=\tfrac{1}{2}\hbar^2(\hbar^{-1}\mathbf{p}-\mathbf{K}_A)\cdot\mathbf{m}_A{}^{-1}\cdot(\hbar^{-1}\mathbf{p}-\mathbf{K}_A), \quad (A.1)$$

and the eigenfunctions of H^0 are the plane waves

$$\psi_k=V^{-\frac{1}{2}}\exp(i\mathbf{k}\cdot\mathbf{r}) \quad (A.2)$$

normalized to the volume V of the crystal.

In the presence of a radiation field whose vector potential is $\mathbf{A}$, one replaces $\mathbf{p}$ by $\mathbf{p}+(e/c)\mathbf{A}$ in the unperturbed Hamiltonian (A.1), and obtains the following perturbation to terms linear in A:

$$H'=\hbar(e/c)\mathbf{A}\cdot\mathbf{m}_A{}^{-1}\cdot(\hbar^{-1}\mathbf{p}-\mathbf{K}_A). \quad (A.3)$$

For present purposes, it will be sufficient to replace $\mathbf{A}$ in (A.3) by one term of the expansion of $\mathbf{A}$ in the normal modes of the radiation field:

$$\mathbf{A}=i\left(\frac{c^2\hbar}{\epsilon V\nu}\right)^{\frac{1}{2}}\boldsymbol{\varepsilon}(\boldsymbol{\nu},\alpha)\eta(h\nu,\alpha)\exp(i\boldsymbol{\nu}'\cdot\mathbf{r}), \quad (A.4)$$

where $\boldsymbol{\nu}$, α, and $\boldsymbol{\varepsilon}(\boldsymbol{\nu},\alpha)$ are, respectively, the vacuum propagation vector, polarization index, and unit polarization vector of the mode; $\boldsymbol{\nu}'=\epsilon^{\frac{1}{2}}\boldsymbol{\nu}$ (ϵ=infrared dielectric constant) is the propagation vector in the crystal; and the destruction operator has the usual matrix element in photon excitation numbers N,

$$(N'|\eta|N)=N^{\frac{1}{2}}\delta(N',N-1). \quad (A.5)$$

The factor $\epsilon^{-\frac{1}{2}}$ on the right-hand side of (A.4) normalizes the field to the interior of the crystal.

Upon inserting the vector potential (A.4) into the perturbing Hamiltonian (A.3) and taking matrix elements between eigenfunctions of the electron (A.2) and of the radiation field [see (A.5)], one obtains the matrix element for photon absorption (superscript a):

$$ {}^aH'_{BA}\equiv(V_\nu{}^a)_{BA}=\gamma_0(\nu,\alpha)\boldsymbol{\varepsilon}(\nu,\alpha)\cdot\mathbf{m}_A{}^{-1}\cdot\mathbf{C}_{BA}, \tag{A.6}$$

$$ \gamma_0(\nu,\alpha)=ie\hbar^2\left(\frac{2\pi n(h\nu,\alpha)}{\epsilon h\nu}\right)^{\frac{1}{2}}, \tag{A.7}$$

$$ \mathbf{C}_{BA}=V^{-1}\int \exp[-i(\mathbf{k}_B-\boldsymbol{\nu}')\cdot\mathbf{r}](\hbar^{-1}\mathbf{p}-\mathbf{K}_A) \times\exp(i\mathbf{k}_A\cdot\mathbf{r})d\mathbf{r}. \tag{A.8}$$

In the coefficient (A.7) the photon density $n(h\nu,\alpha)$ has been written in place of $V^{-1}N(h\nu,\alpha)$.

Since

$$ \hbar^{-1}\mathbf{p}\exp(i\mathbf{k}_A\cdot\mathbf{r})=\mathbf{k}_A\exp(i\mathbf{k}_A\cdot\mathbf{r}), \tag{A.9}$$

Eq. (A.8) becomes

$$ \mathbf{C}_{BA}=(\mathbf{k}_A-\mathbf{K}_A)V^{-1}\int \exp[-i(\mathbf{k}_B-\mathbf{k}_A-\boldsymbol{\nu}')\cdot\mathbf{r}]d\mathbf{r} =(\mathbf{k}_A-\mathbf{K}_A)\delta(\mathbf{k}_B,\mathbf{k}_A+\boldsymbol{\nu}'). \tag{A.10}$$

To a very good approximation in the ranges $T\gtrsim 78°\mathrm{K}$, $\lambda\gtrsim 10\,\mu$ of interest here, $\boldsymbol{\nu}'$ can be ignored in the Kronecker delta of (A.10), so that with (A.10), the matrix element (A.6) becomes effectively

$$ (V_\nu{}^a)_{BA}=\gamma_0(\nu,\alpha)\boldsymbol{\varepsilon}(\nu,\alpha)\cdot\mathbf{m}_A{}^{-1} \cdot(\mathbf{k}_A-\mathbf{K}_A)\delta(\mathbf{k}_B,\mathbf{k}_A). \tag{A.11}$$

The matrix element $(V_\nu{}^e)_{BA}$ for induced photon emission has precisely the same form, except that γ_0 is replaced by $\gamma_0{}^*$.

APPENDIX B

Certain properties of Ge can be used to simplify the computation of the cross section (2.15) when one uses the phonon scattering matrix element (3.1) in conjunction with the forms (3.2) and (3.4) of the interaction vector $\mathbf{Y}$. The discussion of approximations can be made most simply by writing down the scatterer-dependent parts of the cross section (2.15). One puts the absolute square of the matrix element (3.1) into (2.15) and sums on scatterers $(\boldsymbol{\tau},t)$:

$$\begin{aligned}\sum_{\boldsymbol{\tau},t}&|(V_\tau{}^a)_{f0}|^2 \times\delta\{[E(\mathbf{k}_f)-E(\mathbf{k}_0)]/kT-2z_\tau-(-1)^p2x\}+\text{e.t.}\\ &=\sum_{\boldsymbol{\tau},t}\frac{\hbar N(\boldsymbol{\tau},t)}{2\rho V\omega(\tau,t)}\delta(\mathbf{k}_f,\mathbf{k}_0+\boldsymbol{\tau}+\boldsymbol{\kappa}) \times\boldsymbol{\varepsilon}(\boldsymbol{\tau},t)\boldsymbol{\varepsilon}(\boldsymbol{\tau},t):\mathbf{Y}(\boldsymbol{\tau},t)\mathbf{Y}(\boldsymbol{\tau},t)\\ &\times\delta\{[E(\mathbf{k}_f)-E(\mathbf{k}_0)]/kT-2z_\tau-(-1)^p2x\} +\text{e.t.},\end{aligned} \tag{B.1}$$

where the notation (:) means double scalar product, and e.t. means phonon emission terms. The emission terms are obtained from the absorption terms by adding unity to the phonon excitation number $N(\boldsymbol{\tau},t)$ and by changing the signs of $\boldsymbol{\tau}$ in the Kronecker delta and of $2z_\tau=\hbar\omega(\boldsymbol{\tau},t)/kT$ in the Dirac delta function.

Long-wavelength acoustic modes.—The phonon angular frequencies $\omega(\boldsymbol{\tau},t)$ for these scatterers are given to a good approximation by

$$ \omega(\boldsymbol{\tau},t)=v\tau, \tag{B.2}$$

where v is the velocity of sound for longitudinal (v_L) or transverse (v_T) modes. The energy $\hbar\omega(\boldsymbol{\tau},t)$ is then small enough so that $2z_\tau$ can be ignored in the Dirac delta function of (B.1), and so that the usual high-temperature approximation can be made on the equilibrium excitation number $N(\boldsymbol{\tau},t)$:

$$ N(\boldsymbol{\tau},t)\simeq kT/\hbar v\tau. \tag{B.3}$$

Inspection of the appropriate form (3.2) of the interaction vector $\mathbf{Y}$ shows that with (B.2,3) the summand of (B.1) contains $|\boldsymbol{\tau}|$ only in the Kronecker delta. As a result, the Kronecker delta produces only an angular dependence on $\boldsymbol{\tau}=\mathbf{k}_f-\mathbf{k}_0-\boldsymbol{\kappa}$ in the remainder of the summand.

It is also assumed that the unit polarization vector $\boldsymbol{\varepsilon}(\boldsymbol{\tau},3)$ of the longitudinal mode is parallel to $\boldsymbol{\tau}$. This approximation is apparently good[20] over the entire phonon spectrum. With this assumption and the additional assumption that the transverse branches have the same energy $\hbar\omega(\boldsymbol{\tau},t)$ for each $\boldsymbol{\tau}$, one can sum the right-hand side of (B.1) on the two transverse branches to obtain

$$ \sum_{t=1}^{2}\boldsymbol{\varepsilon}(\boldsymbol{\tau},t)\boldsymbol{\varepsilon}(\boldsymbol{\tau},t)=\mathbf{1}-(\boldsymbol{\tau}\boldsymbol{\tau}/\tau^2). \tag{B.4}$$

The derivation of $\sigma_1(\nu)$ and $\sigma_2(\nu)$, Eqs. (3.6) and (3.7), from the cross section (2.15) is now straightforward.

Long-wavelength optical modes.—Near $\boldsymbol{\tau}=0$, the energies $\hbar\omega(\boldsymbol{\tau},t)$ of the three optical modes in Ge are nearly independent of $\boldsymbol{\tau}$ and are all equal to the first-order Raman energy $\hbar\omega_0$. The interaction vector $\mathbf{Y}$ is the constant $\mathbf{B}_0$ [see (3.4)], and the summation on branches $t=4,5,6$ replaces $\boldsymbol{\varepsilon}\boldsymbol{\varepsilon}$ in (B.1) by the unit dyadic. The phonon excitation number $N(\boldsymbol{\tau},t)$ in (B.1) has its exact equilibrium value

$$ N(\boldsymbol{\tau},t)=[\exp(2z_\tau{}^0)-1]^{-1},\quad 2z_\tau{}^0=\hbar\omega_0/kT. \tag{B.5}$$

In the summand of (B.1), the only dependence on $\boldsymbol{\tau}$ occurs in the Kronecker delta itself; the summation on $\boldsymbol{\tau}$ thus yields unity. With these approximations, the cross section (2.15) reduces to the contribution $\sigma_3(\nu)$, Eq. (3.8).

Short-wavelength modes.—The remaining scattering processes are all intervalley processes involving phonons

[20] W. P. Dumke, Phys. Rev. **101**, 531 (1956).

of large momentum $\hbar\tau$ (see Fig. 1). One need only show how these processes simulate transitions caused by long-wavelength optical modes.

Energetic considerations have already been used to demonstrate that electron states of importance to free-carrier absorption in the ranges $\lambda \gtrsim 10\,\mu$, $T<450°\mathrm{K}$, lie rather close to the energy minima, i.e., near the boundaries of the Brillouin zone in Ge. The earlier argument is reinforced by noting that states near the elongated ends of the constant-energy ellipsoids are not nearly as important to absorption as lower mass states. It follows that τ, $\varepsilon(\tau,t)$, and $\omega(\tau,t)$ are nearly independent of (τ,t) for those short-wavelength modes which contribute most to absorption. The above-named quantities can therefore all be replaced by mean values to a good approximation, e.g.,

$$\omega(\tau,t)=\omega(|\mathbf{K}_f-\mathbf{K}_0-\boldsymbol{\kappa}|,\,t). \qquad \text{(B.6)}$$

In these cases, the product $\varepsilon(\tau,t)\cdot\mathbf{B}_n$ can be regarded as the deformation parameter. The resemblance to processes involving long-wavelength optical modes is thus established.

PHYSICAL REVIEW VOLUME 112, NUMBER 3 NOVEMBER 1, 1958

Role of Traps in the Photoelectromagnetic and Photoconductive Effects*

R. N. Zitter
Chicago Midway Laboratories, The University of Chicago, Chicago, Illinois
(Received June 6, 1958)

When carriers recombine through traps, the excess concentrations of mobile electrons and holes are not necessarily characterized by a single lifetime τ. Under the assumption that electrons and holes have separate lifetimes which in general are different, expressions for the steady-state photoelectromagnetic and photoconductive currents are obtained which show that in certain cases the photoelectromagnetic current is determined by a lifetime different from the one determining the photoconductive current. The results of the photoelectromagnetic and photoconductive measurements can be used to evaluate the parameters of any particular model which might be postulated for the recombination process. However, the theoretical treatment of the photoelectromagnetic and photoconductive effects presented here is independent of such models and so can be used as a method for testing their validity.

I. INTRODUCTION

In the course of recent photoelectromagnetic (PEM) and photoconductive (PC) measurements on InSb at 77°K performed at this laboratory, it was found that when the measurements are analyzed according to Kurnick and Zitter's[1] theoretical model, the carrier lifetime deduced from PEM data is much smaller than the lifetime deduced from PC data. This inequality is inconsistent with the theory, which in effect assumes an interband recombination process as opposed to recombination through traps, and therefore predicts that the same value for the lifetime will be obtained in both experiments. Rose[2] has pointed out, however, that if excess carriers are trapped at localized levels in the forbidden band for a significant time before recombining, then one expects the PEM lifetime to be smaller than the PC lifetime.

The purpose of the present paper is to generalize Kurnick and Zitter's model to include the effects of trapping. This will be done in a manner which is independent of any models and statistics of the trapping process itself, i.e., there is no need to mention concentrations of traps, their positions in the forbidden energy gap, etc. The theory will show how the PEM effect, in conjunction with the PC effect, can indicate whether trapping of excess carriers occurs, and, in fact, can provide data from which the parameters of a particular trap model may be inferred. This approach is particularly valuable in those cases where the carrier lifetimes are so short that they can be measured best, if at all, by the steady-state PEM and PC effects.

The equations derived here have been applied to PEM and PC measurements on p-type InSb from 77° to 300°K; the results are to be published shortly.

II. TRAPPING EFFECTS

Over considerable temperature ranges recombination of excess carriers by way of trapping levels in the forbidden energy gap is the predominant recombination mechanism in the bulk semiconductors Ge, Si, and InSb,[3] as well as in many thin-film semiconductors and photoconductive insulators.

For recombination through traps it is instructive to consider the following two limiting cases (which Rose[2] rigorously distinguishes in terms of the position of the Fermi level with respect to the trap level and the trap capture cross sections):

* This research was supported by the U. S. Air Force through the Office of Scientific Research of the Air Research and Development Command.

[1] S. W. Kurnick and R. N. Zitter, J. Appl. Phys. **27**, 278 (1956).

[2] A. Rose, *Proceedings of the Conference on Photoconductivity, Atlantic City, November* 4–6, edited by R. G. Breckenridge *et al.* (John Wiley and Sons, Inc., New York, 1956), p. 17.

[3] G. K. Wertheim, Phys. Rev. **104**, 662 (1956); R. A. Laff and H. Y. Fan, Bull. Am. Phys. Soc. Ser. II, 2, 347 (1957).